Detection of Iron–Oxide Magnetic Nanoparticles Using Magnetic Tunnel Junction Sensors With Conetic Alloy

Z. Q. Lei[1], C. W. Leung[2], L. Li[1], G. J. Li[1], G. Feng[3], A. Castillo[3], P. J. Chen[3], P. T. Lai[1], and P. W. T. Pong[1]

[1]Department of Electrical and Electronic Engineering, The University of Hong Kong, Hong Kong, China
[2]Department of Applied Physics, The Hong Kong Polytechnic University, Hung Hom, Kowloon, Hong Kong, China
[3]Magnetic Materials Group, Metallurgy Division National Institute of Standards and Technology, Gaithersburg, MD 20899-8552 USA

We demonstrated the detection of 20-nm iron–oxide magnetic nanoparticles (MNPs) using Al_2O_3 magnetic tunnel junction sensors (MTJs) with Conetic alloy. Conetic alloy $Ni_{77}Fe_{14}Cu_5Mo_4$ was deposited as the MTJ free layer and pinned layer due to its magnetically soft properties. The magnetoresistance (MR) curves of MTJs with Conetic alloy showed tunneling magnetoresistance of 8.0% with small hysteresis and high linearity in the sensing region, after applying an external magnetic field of 14 Oe along the hard axis. The sensitivity of the MTJ sensors with Conetic alloy was determined to be 0.3%/Oe within a linear region at room temperature. The MNPs of three different concentrations were successfully detected by the shifts of the MR loops of the MTJs, and it was observed that the resistance deviations of the MTJ sensors increased with the logarithm of MNP concentrations. The maximum resistance deviation was 0.16 Ω for an MNP concentration of 20.0 mg/mL. MTJ sensors, together with MNPs, are a promising platform for future biosensor applications, and this paper shows that Conetic alloy is feasible for improving the performance of this platform.

Index Terms—**Iron–oxide magnetic nanoparticles, magnetic sensors, magnetic tunnel junction (MTJ).**

I. Introduction

MAGNETIC tunnel junctions (MTJs) and magnetic nanoparticles (MNPs) have been extensively researched for applications ranging from data storage to biosensing [1], [2]. Magnetoresistive (MR) devices have long been applied in low-field detection due to their superior properties, such as high sensitivity, low-cost, compatibility with complementary metal–oxide semiconductor (CMOS) technology, and room-temperature operation [3]. Giant magnetoresistance (GMR) sensors with a sensitivity of around 1 nanoTesla are now commercially available and MTJ sensors with a sensitivity of 1 picoTesla are under active research [4]. In addition, MNPs can be functionalized for the detection of biological analytes, such as DNAs [5] and proteins [6]. MR sensors, together with MNPs, hold promises for early cancer detection. A potential lung cancer biomarker (interleukin-6) [7] and a colon and breast cancer biomarker (carcinoembryonic antigen) [8] were successfully detected by the detection platform of MR sensors and MNPs. Therefore, a sensor platform enabling the detection of MNPs with MR sensors is critical for biosensor applications [3], [9], and MTJ sensors with MNPs are presently the most encouraging combination.

The basic working principle of MTJ sensors relies on the tunneling magnetoresistance (TMR) effect in thin-film multilayers. Previous studies [3], [4], [10], [11] indicated that the MTJ sensor sensitivity could be enhanced by using soft magnetic thin films. The Conetic alloy (NiFeCuMo) of mu-metal family is magnetically soft and possesses small easy-axis coercivity ($H_{\mathrm{EC}} \sim 10^{-1}$Oe) and large hard-axis magnetic susceptibility ($\chi \sim 10^4 - 10^5$) in single-film and synthetic antiferromagnet multilayer configurations [10], [12], [13]. Its soft magnetic properties can be employed to reduce the coercivity of the MTJ sensors and, thus, enhance the sensitivity [14]. As such, Conetic alloy is a competent alternative magnetic thin film in MTJ stacks for ultra-low magnetic-field detection.

MNPs with a diameter of 20 nm or smaller are recognized as ideal biomolecular labels in biodetection technology [15]. The small size of MNPs is comparable to the dimensions of biomolecules and, thus, increases the density of label binding across the sensor surface. This can greatly enhance the sensitivity and accuracy of quantitative molecular recognition data and actual biorecognition events by conjugating with a few or even single DNA fragments [15]–[17]. It was reported that small MNPs (10–20 nm) are more effective than large magnetic microbeads for targeting intracerebral rat tumors *in vivo* [18]. Therefore, the detection of MNPs with a diameter of 20 nm has a significant impact on the biological applications.

In this paper, we investigated the possibility of detecting iron–oxide MNPs with a diameter of 20 nm utilizing MTJ sensors made with Conetic alloy. The MTJ sensors herein were deposited with Conetic alloy as the magnetic layers. The measurement results indicate that Conetic alloy can largely improve the performance of MTJ sensors and the resulting sensors can be successfully applied for detecting the iron–oxide MNPs.

II. Experiment

The MTJ stack was deposited by magnetron sputtering with a base pressure of 2×10^{-10} torr and its structure was: thermally oxidized silicon substrate/200 Conetic ($Ni_{77}Fe_{14}Cu_5Mo_4$)/10 $Co_{50}Fe_{50}$/10 Al, plasma oxidation, $O_2 = 10^{-3}$ Torr,/10 $Co_{50}Fe_{50}$/25 Conetic ($Ni_{77}Fe_{14}Cu_5Mo_4$)/5 $Co_{50}Fe_{50}$/100 $Ir_{20}Mn_{80}$/70 Ru (units in angstrom). The oxide barrier was

Manuscript received February 21, 2011; revised May 03, 2011, May 13, 2011; accepted May 13, 2011. Date of current version September 23, 2011. Corresponding author: P. W. T. Pong (e-mail: ppong@eee.hku.hk).

Color versions of one or more of the figures in this paper are available online at http://ieeexplore.ieee.org.

Digital Object Identifier 10.1109/TMAG.2011.2157099

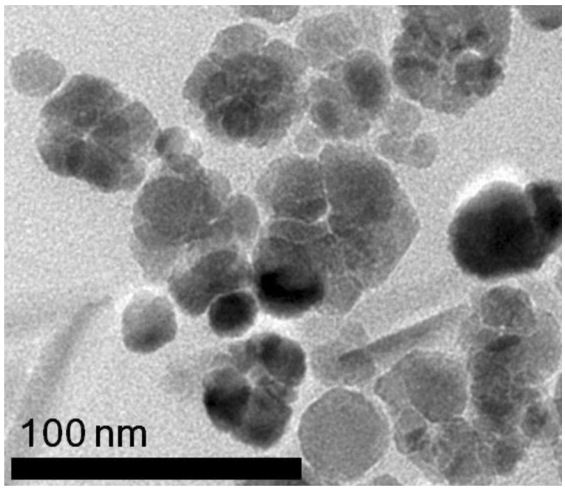

Fig. 1. TEM bright-field image for the iron–oxide MNPs with an average diameter of 20 nm in spherical shape.

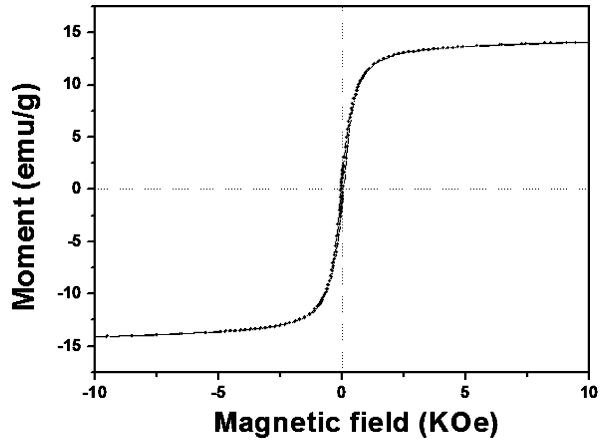

Fig. 2. VSM measurement of the iron–oxide MNPs. The saturation magnetization is 14 emu/g and the coercivity is 45 Oe.

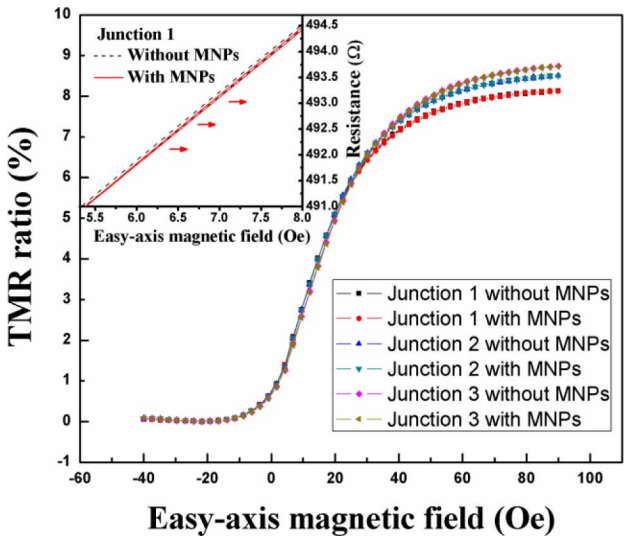

Fig. 3. MR loops of MTJ sensors with Conetic alloy. The data were measured with and without a coating of iron–oxide MNPs using three different concentrations: 0.2 mg/mL for junction 1, 2.0 mg/mL for junction 2, and 20.0 mg/mL for junction 3. The inset is the magnified view of the linear region of the MR loops of junction 1. The arrows indicate the shifting direction of the MR loop.

formed by depositing Al metal and then oxidizing it in oxygen plasma. The stack was annealed at 200 °C for 15 min. The junction area was $20 \times 20\ \mu m^2$, fabricated by self-aligned UV photolithography and etching [12]. The MTJ sensors were mounted on a standard four-probe measurement setup for measuring MR loops, and the entire system was shielded in a mu-metal shielding box to avoid external magnetic-field disturbances. The easy-axis field was provided by a pair of Helmholtz coils ranging from -100 to $+100$ Oe. All of the measurements were conducted at room temperature.

Iron–oxide MNPs (Fe_3O_4, 99.5%, purchased from Nanostructured & Amorphous Materials) were used in this paper. Structural and magnetic characterizations of these MNPs were carried out with transmission electron microscopy (TEM) and vibrating sample magnetometry (VSM), respectively. Fig. 1 shows the TEM image of the iron–oxide MNPs. The iron–oxide MNPs are spherical in shape with an average diameter of 20 nm. The VSM measurement result is presented in Fig. 2. The saturation magnetization of the iron–oxide MNPs is 14 emu/g and the coercivity is 45 Oe. The MNPs were dispersed in ethanol by sonication for 15 mins and vortexed for 15 s at room temperature; three different concentrations of 0.2 mg/mL, 2.0 mg/mL, and 20.0 mg/mL were prepared in this paper. The MTJ sensors were protected by photoresistor with a thickness of 1.6 μm, leaving only the sensing area ($20 \times 20\ \mu m^2$) exposed to ensure that the drop-cast solution was confined within that region. The 0.01-nL MNP solutions with these three concentrations were drop-cast onto three individual MTJ junction surfaces to coat the junction surfaces with the iron–oxide MNPs: 0.2 mg/mL onto junction 1, 2.0 mg/mL onto junction 2, and 20.0 mg/mL onto junction 3. These three junctions were simultaneously fabricated on the same wafer by the same process.

III. Results and Discussion

The fundamental principle of MNP detection by MTJ sensors is to sense the stray magnetic field from the MNPs after being polarized with an external activating magnetic field. The MTJ sensors with Conetic alloy were all biased with an in-plane dc hard-axis field at 14 Oe. This hard-axis magnetic field served for providing initial polarization or magnetization for the MNPs on the MTJs [7], [16]. The biasing field can also be applied in other modes (e.g., vertical dc, in-plane ac, and vertical ac [17]). We herein selected the in-plane dc mode because, besides activating the MNPs, the hard-axis field served two other purposes. On one hand, it was employed to reduce the hysteresis of MTJ sensors. Previous studies have demonstrated that applying an in-plane magnetic field along the hard-axis direction could reduce the hysteretic effect and linearize the MR loops of MTJ sensors [3], [19], [20]. On the other hand, it was helpful for restraining magnetic noise in the MTJ sensors and improving the device sensitivity because the final performance of MTJ sensors is also determined by the basic noise floor [15], [21], [22]. The application of the hard-axis field can enhance the free-layer stability and reduce the magnetic noise by limiting magnetization fluctuation in the magnetic layers of MTJs.

The MR loops of the MTJ sensors with Conetic alloy were measured before and after the coating of the iron–oxide MNPs,

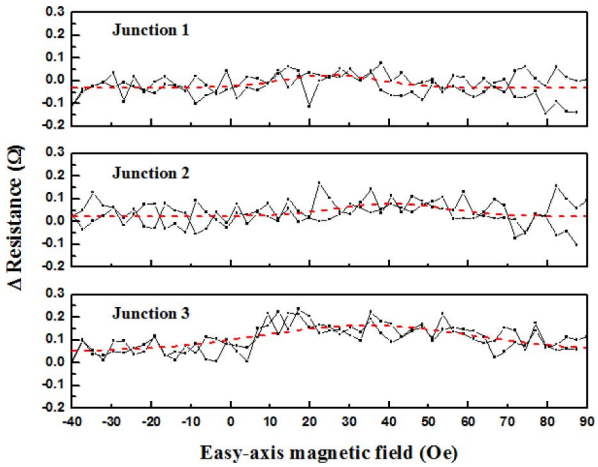

Fig. 4. Plots of the resistance deviations ΔR of MTJ sensors after being coated with iron–oxide MNPs against the easy-axis field (black solid line). The fitting curve (red dashed line) illustrates that the maximum resistance deviations of the three junctions are 0.02, 0.08, and 0.16 Ω, respectively.

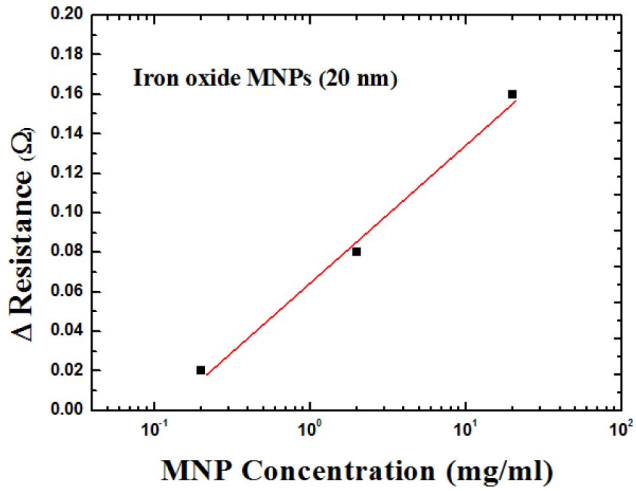

Fig. 5. Graph of MTJ sensor resistance deviations ΔR versus iron–oxide MNP concentrations. The fitting curve (solid line) designates that the resistance deviation of the MTJ sensor changes with the logarithm of the MNP concentration.

and the results are shown in Fig. 3. All curves exhibited tunneling magnetoresistance (TMR) of 8.0% and a sensitivity of 0.3%/Oe without hysteresis under the hard-axis bias. The coating of iron–oxide MNPs on the MTJ junction surfaces shifted the MR loops from their original positions to the right. The inset of Fig. 3 shows the magnified linear region of the MR loops of Junction 1 as an example to illustrate the shift. Fig. 4 plots the resistance deviations ΔR of the MTJ sensors after the coating of the iron–oxide MNPs against the easy-axis field. From the dashed fitting curves, it can be observed that the maximum resistance deviations of the three junctions are 0.02 Ω (junction 1), 0.08 Ω (junction 2), and 0.16 Ω (junction 3), respectively. The relation between the resistance deviation of the MTJ sensor after coated with MNPs and the MNP concentration is plotted in Fig. 5. The resistance deviation of the MTJ sensor changes with the logarithm of the concentration of iron–oxide MNPs. This result consists with the previous studies reported by other groups [7], [23], [24]. As such, the concentration of MNPs can be deduced through the resistance deviation of the MTJ sensors.

IV. Conclusion

Conetic alloy was deposited as the magnetic layers of Al_2O_3 MTJ sensors. The MTJ sensors exhibited a TMR of 8.0% and a sensitivity of 0.3%/Oe. The hysteresis of the MR loop was eliminated by applying a hard-axis field of 14 Oe. The detection of iron–oxide MNPs was achieved by drop-casting the MNP solution onto the surfaces of the MTJs sensing area with three different concentrations of 0.2, 2.0, and 20.0 mg/mL. The coating of MNPs shifted the MR loops, and the MTJ resistance deviations after coating MNPs were 0.02, 0.08, and 0.16 Ω, respectively. These data show that the presence of 20-nm MNPs can be detected by MTJ sensors with Conetic alloy, and the concentration of MNPs can be deduced from the magnitude of MTJ resistance deviations.

Acknowledgment

This work was supported by the Seed Funding Program for Basic Research from the University of Hong Kong and the RGC–GRF grant (HKU 7049/11P).

References

[1] S. Sun, C. B. Murray, D. Weller, L. Folks, and A. Moser, "Monodisperse FePt nanoparticles and ferromagnetic FePt nanocrystal superlattices," *Science*, vol. 287, pp. 1989–1992, 2000.

[2] C. Alexiou, A. Schmidt, R. Klein, P. Hulin, C. Bergemann, and W. Arnold, "Magnetic drug targeting: Biodistribution and dependency on magnetic field strength," *J. Magn. Magn. Mater.*, vol. 252, pp. 363–366, 2002.

[3] P. P. Freitas *et al.*, "Magnetoresistive sensors," *J. Phys. Condens. Matter*, vol. 19, p. 165221, 2007.

[4] A. Edelstein, "Advances in magnetometry," *J. Phys. Condens. Matter*, vol. 19, p. 165217, 2007.

[5] S. G. Grancharov, H. Zeng, S. Sun, S. X. Wang, S. O'Brien, C. B. Murray, J. R. Kirtley, and G. A. Held, "Bio-functionalization of monodisperse magnetic nanoparticles and their use as biomolecular labels in a magnetic tunnel junction based sensor," *J. Phys. Chem. B*, vol. 109, pp. 13030–13035, 2005.

[6] Y. Li, B. Srinivasan, Y. Jing, X. Yao, M. A. Hugger, J.-P. Wang, and C. Xing, "Nanomagnetic competition assay for low-abundance protein biomarker quantification in unprocessed human sera," *J. Amer. Chem. Soc.*, vol. 132, pp. 4388–4392, 2010.

[7] B. Srinivasan, Y. Li, Y. Jing, Y. Xu, X. Yao, C. Xing, and J.-P. Wang, "A detection system based on giant magnetoresistive sensors and high-moment magnetic nanoparticles demonstrates zeptomole sensitivity: Potential for personalized medicine," *Angew. Chem. Int. Ed.*, vol. 48, pp. 2764–2767, 2009.

[8] R. S. Gaster, D. A. Hall, C. H. Nielsen, S. J. Osterfeld, H. Yu, K. E. Mach, R. J. Wilson, B. Murmann, J. C. Liao, S. S. Gambhir, and S. X. Wang, "Matrix-insensitive protein assays push the limits of biosensors in medicine," *Nat. Med.*, vol. 15, pp. 1327–1332, 2009.

[9] W. Shen, B. D. Schrag, M. J. Carter, J. Xie, C. Xu, S. Sun, and G. Xiao, "Detection of DNA labeled with magnetic nanoparticles using MgO-based magnetic tunnel junction sensors," *J. Appl. Phys.*, vol. 103, pp. 07A306–3, 2008.

[10] W. F. Egelhoff, R. D. McMichael, C. L. Dennis, M. D. Stiles, F. Johnson, A. J. Shapiro, B. B. Maranville, and C. J. Powell, "Soft magnetic layers for low-field-detection magnetic sensors," *Thin Solid Films*, vol. 505, pp. 90–92, 2006.

[11] P. Joyoung and Y. Haein, "Designing the composition of amorphous free layer of a magnetic tunnel junction," *IEEE Trans. Magn.*, vol. 45, no. 6, pp. 2413–2416, Jun. 2009.

[12] P. W. T. Pong and W. F. Egelhoff, "Fabrication strategies for magnetic tunnel junctions with magnetoelectronic applications," *Proc. SPIE*, vol. 6645, pp. 66451V–11, 2007.
[13] J.-G. Choi, D.-G. Hwang, J.-R. Rhee, and S.-S. Lee, "Comparison of the soft magnetic properties of permalloy and conetic thin films," *J. Magn. Magn. Mater.*, vol. 322, pp. 2191–2194, 2010.
[14] Z. Q. Lei, G. J. Li, W. F. Egelhoff, P. T. Lai, and P. W. T. Pong, "Magnetic tunnel junctions sensors with conetic alloy," *IEEE Trans. Magn.*, vol. 47, no. 3, pp. 714–717, Mar. 2011.
[15] Q. A. Pankhurst, J. Connolly, S. K. Jones, and J. Dobson, "Applications of magnetic nanoparticles in biomedicine," *J. Phys. D: Appl. Phys.*, vol. 36, p. R167, 2003.
[16] D. L. Graham, H. A. Ferreira, and P. P. Freitas, "Magnetoresistive-based biosensors and biochips," *Trends Biotechnol.*, vol. 22, pp. 455–462, 2004.
[17] G. Li, S. Sun, R. J. Wilson, R. L. White, N. Pourmand, and S. X. Wang, "Spin valve sensors for ultrasensitive detection of superparamagnetic nanoparticles for biological applications," *Sens. Actuators, A*, vol. 126, pp. 98–106, 2006.
[18] S. K. Pulfer, S. L. Ciccotto, and J. M. Gallo, "Distribution of small magnetic particles in brain tumor-bearing rats," *J. Neuro-Oncol.*, vol. 41, pp. 99–105, 1999.
[19] M. Tondra, J. M. Daughton, D. Wang, R. S. Beech, A. Fink, and J. A. Taylor, "Picotesla field sensor design using spin-dependent tunneling devices," *J. Appl. Phys.*, vol. 83, pp. 6688–6690, 1998.
[20] X. Liu, C. Ren, and G. Xiao, "Magnetic tunnel junction field sensors with hard-axis bias field," *J. Appl. Phys.*, vol. 92, pp. 4722–4725, 2002.
[21] D. Mazumdar, X. Liu, B. D. Schrag, M. Carter, W. Shen, and G. Xiao, "Low frequency noise in highly sensitive magnetic tunnel junctions with (001) MgO tunnel barrier," *Appl. Phys. Lett.*, vol. 91, pp. 033507–3, 2007.
[22] N. Smith, J. A. Katine, J. R. Childress, and M. J. Carey, "Thermal and spin-torque noise in CPP (TMR and/or GMR) read sensors," *IEEE Trans. Magn.*, vol. 42, no. 2, pt. 1, pp. 114–119, Feb. 2006.
[23] J. Schotter, P. B. Kamp, A. Becker, A. Pühler, G. Reiss, and H. Brückl, "Comparison of a prototype magnetoresistive biosensor to standard fluorescent DNA detection," *Biosens. Bioelectron.*, vol. 19, pp. 1149–1156, 2004.
[24] W. Shen, B. D. Schrag, M. J. Carter, and G. Xiao, "Quantitative detection of DNA labeled with magnetic nanoparticles using arrays of MgO-based magnetic tunnel junction sensors," *Appl. Phys. Lett.*, vol. 93, pp. 033903–3, 2008.